Air Quality Improvement in a Megacity: Implications from 2015 Beijing Parade Blue Pollution-Control Actions

Wen Xu[1,a,#], Wei Song[2,#], Yangyang Zhang[1,#], Xuejun Liu[1,*], Lin Zhang[3], Yuanhong Zhao[3], Duanyang Liu[4], Aohan Tang[1], Daowei Yang[1], Dandan Wang[1], Zhang Wen[1], Yuepeng Pan[5], David Fowler[6], Jeffrey L. Collett Jr.[7], Jan Willem Erisman[8], Keith Goulding[9], Yi Li[10], Fusuo Zhang[1]

[1]College of Resources and Environmental Sciences, Center for Resources, Environment and Food Security, Key laboratory of Plant-Soil Interactions of MOE, China Agricultural University, Beijing 100193, China

[2]Institute of Surface-Earth System Science, Tianjin University, Tianjin, 300072, China

[3]Laboratory for Climate and Ocean-Atmosphere Studies, Department of Atmospheric and Oceanic Sciences, School of Physics, Peking University, Beijing 100871, China

[4]Jiangsu Meteorological Observatory, Nanjing 210008, China

[5]State Key Laboratory of Atmospheric Boundary Layer Physics and Atmospheric Chemistry (LAPC), Institute of Atmospheric Physics, Chinese Academy of Sciences, Beijing 100029, China

[6]Centre for Ecology and Hydrology Edinburgh, Bush Estate, Penicuik, Midlothian EH26 0QB, UK

[7]Department of Atmospheric Science, Colorado State University, Fort Collins, CO 80523, USA

[8]Louis Bolk Institute, Hoofdstraat 24, 3972 LA Driebergen, The Netherlands

[9]The Sustainable Soil and Grassland Systems Department, Rothamsted Research, West Common, Harpenden, Hertfordshire, AL5 2JQ, UK

[10]Arizona Department of Environmental Quality, Phoenix, AZ, 85007, USA

[a]Current address: State Key Laboratory of Urban and Regional Ecology, Research Center for Eco-Environmental Sciences, Chinese Academy of Sciences, Shuangqing Road 18, Haidian District, Beijing 100085, China

[#] Equal contribution; [*] Corresponding author (Email: liu310@cau.edu.cn)

Abstract:

The implementation of strict emission control measures in Beijing and surrounding regions during the 2015 China Victory Day Parade provided a valuable opportunity to investigate related air quality improvements in a megacity. We measured NH_3, NO_2 and $PM_{2.5}$ at multiple sites in and outside Beijing and summarized concentrations of $PM_{2.5}$, PM_{10}, NO_2, SO_2 and CO in 291 cities across China from a national urban air quality monitoring network between August and September 2015. Consistently significant reductions of 12-35% for NH_3 and 33-59% for NO_2 in different areas of Beijing city during the emission control period (referred to as the Parade Blue period) were observed compared with measurements in the pre- and

post-Parade Blue periods without emission controls. Average NH_3 and NO_2 concentrations at sites near traffic were strongly correlated and showed positive and significant responses to traffic reduction measures, suggesting that traffic is an important source of both NH_3 and NO_x in urban Beijing. Daily concentrations of $PM_{2.5}$ and secondary inorganic aerosol (sulfate, ammonium, and nitrate) at the urban and rural sites both decreased during the Parade Blue period. During (after) the emission control period, concentrations of $PM_{2.5}$, PM_{10}, NO_2, SO_2 and CO from the national city-monitoring network showed the largest decrease (increase) of 34-72% (50-214%) in Beijing, a smaller decrease (a moderate increase) of 1-32% (16-44%) in emission control regions outside Beijing, and an increase (decrease) of 6-16% (-2-7%) in non-emission control regions of China. Integrated analysis of modeling and monitoring results demonstrated that emission control measures made a major contribution to air quality improvement in Beijing compared with a minor contribution from favorable meteorological conditions during the Parade Blue period. These results show that controls of secondary aerosol precursors (NH_3, SO_2 and NO_x) locally and regionally are key to curbing air pollution in Beijing and probably in other mega cities worldwide.

Introduction

China's economy has made great advances over the last three decades. Its gross domestic production (GDP) ranked fifteenth in the world in 1978 but has risen to second place since 2010. During this period, environmental pollution has greatly increased, including soil, water and air pollution (Chan et al., 2008; Guo et al., 2010; Chen et al., 2014; Lu et al., 2015), which has become a major issue for the country. The Chinese government and people have grown particularly concerned about reducing air pollution since the large-scale haze pollution that occurred in China in January 2013. This episode affected an area of approximately 1.3 million km^2 and 800 million people (Huang et al., 2014). It led to serious human health problems and forced the Chinese government to address the problem of very large exposures of the

Chinese population to $PM_{2.5}$ (particulate matter ≤ 2.5 μm in aerodynamic diameter) pollution. For example, compared with a similar winter period without haze pollution (daily child patients < 600), more than 7000 daily child patients were reported in Beijing Children's Hospital during the smog period in January 2013 (http://qnck.cyol.com/html/2014-01/01/nw.D110000qnck_20140101_1-28.htm). In response to this the 'Atmospheric Pollution Prevention and Control Action Plan' was implemented by the Chinese government in September 2013, aiming to reduce $PM_{2.5}$ in Beijing by at least 25% from the 2012 level by 2017.

Many industrialized megacities have experienced severe air pollution, such as Los Angeles during the 1940s-1970s (Haagen-Smit, 1952; Parrish et al., 2011), Mexico city in the 1980s (Parrish et al., 2011), and London in the 1950s (Davis et al., 2002). In these megacities, however, enormous progress in improving air quality has been achieved with the implementation of various emission control strategies over recent decades, despite rapid population growth and urbanization. According to Parrish et al. (2011), first stage smog alerts in Los Angeles have decreased from some 200 per year in the 1970s to about 10 per year now, and concentrations of air pollutants in Mexico City have been reduced substantially over the past decades. Also, air quality is now much better in London, with mean annual PM_{10} (particulate matter ≤10 μm in aerodynamic diameter) levels closer to 30 μg m^{-3} than the 300 μg m^{-3} fifty years ago (and approx. 3000 μg m^{-3} in December 1952) (Davis et al., 2002).

Beijing, the capital of China, is one of the largest megacities in the world with 22 million inhabitants and an area of 16800 square kilometers. The city is enclosed by the Yanshan Mountains to the north and Taihang Mountains to the west. Its fan-shaped topography permits efficient southerly transport of pollutants to Beijing, which reduces air quality (Chen et al., 2015). A 70^{th} anniversary victory parade was held in Beijing on 3 September 2015 to commemorate the conclusion of the second Sino-Japanese War and the end of World War II. The Chinese government imposed a series of strict and urgent air pollutant emission-reduction measures to improve air quality during what has been called the 'Parade Blue' period, from 20 August to 3

September 2015, in Beijing and surrounding regions (including Tianjin City, Inner Mongolia Autonomous Region, Hebei, Shandong, Shanxi, and Henan Provinces) to guarantee better air quality in the city. During this period, motor vehicles (except taxis and buses) with even or odd registration numbers were banned on alternate days, 1927 industrial enterprises had to limit production or were shut down, and hundreds of construction sites in Beijing were closed, reducing air pollutant emissions by 40% (http://gongyi.sohu.com/20150826/n419765215.shtml). For all seven of the cities, provinces and autonomous regions, air pollutant emissions during the Parade Blue period were decreased by 30% through a variety of reduction measures (http://news.sohu.com/20150819/n419198051.shtml). No additional pollution control measures were taken in other regions of China (outside Beijing and surrounding regions) during this period.

Previous studies have attempted to quantify the role of short-term pollutant emission control measures in air quality improvement in Beijing during the 2008 Olympics (Wang et al., 2009, 2010; Shen et al., 2011) and the 2014 Asia-Pacific Economic Cooperation (APEC) meeting (Chen et al., 2015). In addition, Tang et al. (2015) reported that local emissions are the key factors determining the formation and development of air pollution in the Beijing area. Ianniello et al. (2010) inferred that traffic may be an important emission source of NH_3 in Beijing. However, the above studies did not systematically answer the three following questions: what were (1) the contribution of ammonia (NH_3) sources to urban $PM_{2.5}$ pollution; and (2) the relative roles of pollution control measures and weather conditions in air quality improvement? The present study attempts to examine these important topics by taking advantage of the implementation of emission controls for the 70^{th} anniversary victory parade. We present results showing changes in concentrations of atmospheric pollutants (i.e., NH_3, NO_2, $PM_{2.5}$ and associated inorganic water-soluble ions (WSIs)) before, during, and after the Parade Blue period, obtained from *in situ* measurements at thirty-one sites in and outside Beijing. In addition, we compare the Chinese Ministry of Environmental Protection officially released daily concentrations of

$PM_{2.5}$, PM_{10}, NO_2, SO_2 and CO at 291 cities in China during the same period. The first results from the analysis of this extensive dataset reveal clear effects of the Parade Blue emission reduction measures on air quality improvement and provide a scientific basis for demonstrating the effectiveness of such control measures for air pollution in mega cities.

2 Materials and methods

2.1 Site selection and description

Thirty-one air pollution monitoring sites have been established in and outside Beijing municipality, with longitudes ranging from 115.02 ºE to 118.20 ºE and latitudes from 36.84 ºN to 40. 34 ºN (**Fig. 1**). The 28 monitoring sites in Beijing municipality are grouped into road and non-road sites to better distinguish the impacts of control measures on sites near traffic. A brief description of all the sites is given below. Detailed information, including specific sampling site, site type, and potential emission sources for each site, is listed in **Table S1** in the Supplement.

In Beijing: Sixteen roadside monitoring sites are homogeneously distributed at the edges of three major roads, including four sites each on the 3rd and 4th ring roads, and eight sites on the 5th ring road. Additional road sites (sites 26 to 28) are in northwest rural regions near the Yanshan mountains. Site 26 is located at the edge of the Badaling highway, about 46 km northwest of the center of Beijing. Sites 27 and 28 are located, respectively, inside (100 m from the exit) and outside (30 m from the entrance) the Badaling Highway Tunnel (1091.2 m long), which has two traffic tunnels with one lane in each. The road sites were strongly and directly influenced by vehicle emissions. Nine non-road sites were chosen over a wide area, extending from an urban area (site 1) near the city center, through suburban areas (sites 6, 11, 12 and 13) between the 3rd and 5th ring roads, and ending in rural areas (sites 22 to 25) between the northwest 5th and 6th ring roads. These are likely to be polluted by emissions from various sources, including dense housing, industry, cropland, small villages, etc.

Outside Beijing: Site 29 is located in a rural area of Yucheng city, Shandong

province. Site 30 is located in Quzhou county, Hebei province, which is a typical rural agricultural site with a recently constructed industrial district. Site 31 is a regional background site located on Changdao island, Shandong province.

2.2 Sampling procedure and sample analysis

Atmospheric NH_3, NO_2 and $PM_{2.5}$ were measured from 3 August to 30 September 2015. The period can be divided into three phases: (1) 3-19 August (named pre-Parade Blue period), (2) 20 August-3 September (Parade Blue period), and (3) 4-30 September (post-Parade Blue period). The sampling durations, measured pollutants and number of samples for all the sites during each phase are summarized in **Table S1** in the Supplement. The measurements of NH_3, NO_2 and $PM_{2.5}$ were not concurrently made at most sites due to a shortage of manpower and samplers, but the corresponding sampling sites together covered the major emission sources of measured pollutants. Methods for sampling gases and $PM_{2.5}$ are briefly presented below. For further details of the methodology the reader is referred to relevant previous publications (Xu et al., 2014, 2015, 2016).

Gaseous NH_3 and NO_2: NH_3 samples were collected using ALPHA passive samplers (Adapted Low-cost High Absorption, provided by the Centre for Ecology and Hydrology, Edinburgh, UK) and NO_2 samples using Gradko diffusion tubes (Gradko International Limited, UK). At each site, three ALPHA samplers and/or three NO_2 tubes were deployed under a PVC shelter (2 m above the ground) to protect the samplers from rain and direct sunlight (Pictures for 4 selected road sites are shown in **Fig. S1** of the Supplement). The samplers were exposed for 7 to 14 days during the three study phases. NH_3 was extracted with high-purity water (18.2 MΩ) and analyzed using a continuous-flow analyzer (Seal AA3, Germany). NO_2 samples, also extracted with high-purity water, were analyzed using a colorimetric method by absorption at a wavelength of 542 nm. More details of the passive samplers and their laboratory preparation and analysis can be found in Xu et al. (2014, 2015).

Airborne $PM_{2.5}$: 24-h $PM_{2.5}$ samples were collected on 90 mm quartz fiber filters (Whatman QM/A, Maidstone, UK) using medium-volume samplers (TH-150CIII,

Tianhong Co., Wuhan, China), at a flow rate of 100 L min^{-1}. The $PM_{2.5}$ mass was determined using the standard gravimetric method, and one quarter of each $PM_{2.5}$ sample was ultrasonically extracted with 10 ml high-purity water for 30 min, with the extract being filtered by a syringe filter (0.45 μm, Tengda Inc., China). The water-soluble cations (NH_4^+, Na^+, Ca^{2+}, K^+, Mg^{2+}) and anions (NO_3^-, SO_4^{2-}, F^-, Cl^-) in the extract were analyzed using Dionex-600 and Dionex-2100 Ion Chromatographs (Dionex Inc., Sunnyvale, CA, USA), respectively (Zhang et al., 2011; Tao et al., 2014).

2.3 Quality assurance/ Quality control (QA/QC)

All samples were prepared and measured in the Key Laboratory of Plant-Soil Interactions, Chinese Ministry of Education, China Agricultural University, which has a complete and strict quality control system. Three field (travel) blanks were prepared for each batch of samples and analyzed together with those samples. All reported concentrations of gases and $PM_{2.5}$ mass and ion concentrations are corrected for the blanks. The detection limits were 0.01-0.02 mg L^{-1} for the measured ions. The measurement precisions were in the range of 5-10% for NH_3, NO_2, $PM_{2.5}$ mass and water soluble ion concentrations. Quality assurance was routinely (once every 15-20 samples) checked using standard (designed specific concentrations of various ions) samples during sample analysis.

2.4 Other data collection

The 24-h (daily) average concentrations of $PM_{2.5}$, PM_{10}, NO_2, SO_2 and CO measured in 291 cities across China (including Beijing city, surrounding 63 cities in emission control regions (hereafter termed to emission control regions (excluding Beijing)), and 227 cities in other regions of China (hereafter referred to as non-emission control regions) during the Pre-Parade Blue, Parade Blue and post-Parade periods were downloaded from the Ministry of Environmental Protection (MEP) of China (http://www.mep.gov.cn). These data for each city are summarized in **Tables S2-6** in the Supplement. For Beijing city, each pollutant's daily individual Air Quality Index (AQI) during the above three periods was calculated from the 24-h average

concentration. The highest individual AQI was selected and used as the daily AQI. An AQI of 0-50, 51-100, 101-150, and 151-200 is classified as “excellent”, “good”, “slightly polluted” and “moderately polluted”, respectively. Details of the calculations of AQI and the associated classification of air quality are given in the Chinese Technical Regulations on AQI (MEPC, 2012).

Daily meteorological data in the above mentioned 291 cities for wind speed (WS), temperature (*T*), and relative humidity (RH) during the Parade Blue period and non-Parade Blue periods (the pre- and post-Parade Blue periods) were obtained from Weather Underground (http://www.underground.com). The daily precipitation and half-hourly wind speed and direction were measured in Beijing city. The NCEP/NCAR global reanalysis meteorological data (including daily wind speed, wind direction, sea surface pressure and precipitation) during the same periods were provided by the NOAA/OAR/ESRL PSD, Boulder, Colorado, USA, from their website (http://www.esrl.noaa.gov/psd). The daily mean atmospheric mixing layer height (MLH) in Beijing during the period from 3 August to 30 September 2015 was calculated using the method described in Holzworth (1964, 1967).

2.5 Back trajectories and statistical analysis

The 72-h (3-day) backward trajectories arriving at Beijing were calculated four times a day (00:00, 06:00, 12:00, and 18:00 UTC) at 100 m height using the Hybrid Single Particle Lagrangian Integrated Trajectory (HYSPLIT-4, NOAA) 4.9 model (Draxler and Hess, 1997). Meteorological data with a resolution of 0.5° × 0.5° were input from the Global Data Assimilation System (GDAS) meteorological data archives of the Air Resource Laboratory, National Oceanic and Atmospheric Administration (NOAA). The trajectories were then grouped into four clusters during each period using cluster analysis based on the total spatial variance (TSV) method (Draxler et al., 2012). Values of NH_3, NO_2, $PM_{2.5}$ and ion concentrations per study phase at the sampling sites are shown as the mean ± standard error (SE). Temporal differences between study phases of concentrations of measured gases (NH_3 and NO_2) and the

MEP of reported pollutants (i.e. $PM_{2.5}$, PM_{10}, NO_2, SO_2 and CO) were investigated using paired t-tests while those of measured $PM_{2.5}$ mass and associated ionic components were investigated using a non-parametric Mann-Whitney U test. All statistical analyses were performed using SPSS11.5 (SPSS Inc., Chicago, IL, USA). Statistically significant differences were set at $p < 0.05$ unless otherwise stated.

3. Results

3.1 Concentrations of gaseous NH_3 and NO_2

Ambient NH_3 concentrations varied greatly during the pre-Parade Blue, Parade Blue and post-Parade Blue periods, with values of 8.2-31.7, 7.8-50.7 and 7.4-40.2 μg m^{-3}, respectively (**Fig. 2A a**). The average NH_3 concentrations during the three periods for the sites inside the 6th ring road (including road sites (RS) on the 3rd, 4th and 5th ring roads and non-road sites (NRS)), outside the 6th ring road but in Beijing and outside Beijing, are shown in **Fig. 2A b and c**. The mean NH_3 concentration inside the 6th ring road was significantly smaller (by 13%) during the Parade Blue period compared with the mean during the post-Parade Blue period (20.2 ± 1.2 μg m^{-3} versus 23.3 ± 1.8 μg m^{-3}); further, on all three ring roads reductions (23 to 35%) of the mean during the Parade Blue period were statistically significant while at the non-road sites a small non-significant increase (15%) in the mean was observed (**Fig. 2A c**). The mean NH_3 concentration outside the 6th ring road was 12% smaller in the Parade Blue period than in the post-Parade Blue period (21.4 ± 6.0 μg m^{-3} versus 24.3 ± 9.3 μg m^{-3}), whereas outside Beijing, non-significant increases (on average 80%) in the mean occurred during the Parade Blue period (26.7 ± 12.6 μg m^{-3}) compared with those during the pre- and post-Parade Blue periods (19.9 ± 6.2 and 11.8 ± 2.3 μg m^{-3}, respectively).

Ambient NO_2 concentrations ranged from 21.5 to 227.7, 14.1 to 258.8, and 15.7 to 751.8 μg m^{-3} during the pre-Parade Blue, Parade Blue and post-Parade Blue periods, respectively (**Fig. 2B a**). The mean NO_2 concentrations at the sites inside the 6th ring road (including road sites on the 5th ring road and NRS), outside the 6th ring road and

outside Beijing during the three periods are shown in **Fig. 2B b and c**. Inside the 6th ring road, the mean concentration during the Parade Blue period (78.7 μg m^{-3}) was 42% and 35% lower (p<0.01) than the means during the pre- and post-Parade Blue periods (135.7 ± 21.8 and 121.0 ± 16.5 μg m^{-3}, respectively). For the 5th ring RS and NRS, most reductions (33~42%) in the mean during the Parade Blue period were also highly significant (p<0.01). Inside the 6th ring road, a large non-significant reduction (59%) in the mean concentration occurred during the Parade Blue period compared with the post-Parade Blue period (183.5 ± 49.1 versus 443.4 ± 173.3 μg m^{-3}). Outside Beijing, the change in the mean during the Parade Blue period (23.7 ± 3.6 μg m^{-3}) was small and non-significant when compared with the means during the pre- and post-Parade periods (27.5 ± 4.5 and 18.5 ± 1.7 μg m^{-3}, respectively).

3.2 Concentrations of $PM_{2.5}$ and its chemical components

A statistical analysis of concentrations of $PM_{2.5}$ mass and associated inorganic WSIs at sites 22, 29 and 30 in the three periods is presented in **Table 1**. Daily $PM_{2.5}$ concentrations ranged from 4.2 to 123.6, 15.4 to 116.0, and 12.4 to 170.7 μg m^{-3} at sites 22, 29 and 30, respectively. At sites 22 and 29, mean $PM_{2.5}$ concentrations during the Parade Blue period decreased significantly (by 49% and 40%, respectively) compared with the means during the pre-Parade Blue period, and increased again during the post-Parade Blue period (57% and 3%, respectively) compared with the means during the Parade Blue period. At site 30, a 24% reduction in mean $PM_{2.5}$ concentrations occurred during the Parade Blue period compared with the pre-Parade Blue period and a 103% increase during the post-Parade Blue period. Secondary inorganic aerosols (SIA) (sum of NH_4^+, NO_3^- and SO_4^{2-}) were major components of $PM_{2.5}$, with average contributions of 24%, 41% and 32% to the daily average $PM_{2.5}$ mass at sites 22, 29 and 30, respectively. As with $PM_{2.5}$ concentrations, concentrations of all the WSIs (except for Cl^-) at site 22 decreased significantly during the Parade Blue period compared with the pre- and/or post-Parade Blue periods. Analogous behavior also occurred at sites 29 and 30 for

297 concentrations of NO_3^-, NH_4^+ and SO_4^{2-} but not for those of most of other ions (e.g.
298 Ca^{2+}, K^+, F^-, Na^+).
299
300 *3.3 Daily mean pollutant concentrations from MEP*
301 Daily mean concentrations of the five major pollutants ($PM_{2.5}$, PM_{10}, NO_2, SO_2 and
302 CO) at 291 cities in China, divided into three groups of Beijing, cities in emission
303 control regions (excluding Beijing) and cities in non-emission control regions, are
304 summarized in **Fig. 3**. Average concentrations of $PM_{2.5}$, PM_{10}, NO_2, SO_2 and CO
305 during the Parade Blue period were highly significantly (p<0.01) decreased in
306 Beijing, with reductions of 72%, 67%, 39%, 34% and 39%, respectively, compared
307 with the pre-Parade Blue period. $PM_{2.5}$ concentrations in Beijing, for example,
308 remained below 20 μg m^{-3} for 14 consecutive days in the Parade Blue period (for
309 comparison: the WHO and China's (first-grade) thresholds for daily $PM_{2.5}$
310 concentrations are 25 and 35 μg m^{-3}, respectively). The daily $PM_{2.5}$ concentrations in
311 Beijing in the pre-Parade Blue period averaged 59 μg m^{-3}. Concentrations of $PM_{2.5}$,
312 PM_{10} and SO_2 in the Parade Blue period were also significantly (p<0.05) decreased
313 in cities in emission control regions (excluding Beijing), with reductions of 32%,
314 29% and 7%, respectively, while concentrations of NO_2 and CO did not show
315 statistically significant changes (p>0.05). After the Parade Blue period,
316 concentrations of the five major pollutants in Beijing and surrounding regions
317 rebounded quickly, with significant increases of 50-214%, and 16-44%, respectively.
318 In cities in other regions, by contrast, where no additional emission reduction
319 measures were taken, concentrations of $PM_{2.5}$, PM_{10}, NO_2, SO_2 and CO remained
320 stable or were significantly (p<0.05) higher during the Parade Blue period compared
321 with the pre- and post-Parade Blue periods.
322
323 **4. Discussion**
324 *4.1 Effect of emission controls on air quality*

The statistical analyses (**Fig. 3**) show that, by taking regional emission controls during the Parade Blue period, daily concentrations of the five reported pollutants ($PM_{2.5}$, PM_{10}, NO_2, SO_2 and CO) in Beijing city and surrounding other cities in the six provinces were decreased by various but statistically significant amounts, in sharp contrast to increases in cities in other parts of China where no additional emission controls were imposed. This shows the effectiveness of the pollution controls and suggests that air quality improvement was directly related to the reduction intensities of pollutant emissions (e.g., air pollution control effects ranked by Beijing (largest reduction) > emission control regions surrounding Beijing (moderate reduction) > other regions (no reduction) in China). Another way of quantifying the effect of the additional control measures for Beijing uses the Air Quality Index (MEPC, 2012). On the basis of the calculated air quality index (AQI, **Fig. 4**), defined "good" and polluted days (i.e. "slightly polluted" and "moderately polluted") altogether accounted for 89% during the pre-Parade Blue period, and 70% during the post-Parade Blue period. The primary pollutant was $PM_{2.5}$ for 82% and 63% of these days during the Pre- and post-Parade Blue periods, respectively. In contrast, almost all of the days during the Parade Blue period were defined as "excellent". Thus improved air quality-as represented by the AQI during the Parade Blue period was mainly attributed to the additional control of $PM_{2.5}$ precursors.

Results from the MEP of source apportionment of $PM_{2.5}$ for Beijing (http://www.bj.xinhuanet.com/bjyw/2014-04/17/c_1110289403.htm) showed that 64-72% of atmospheric $PM_{2.5}$ during 2012-2013 was generated by emissions from local sources, of which the biggest contributor was vehicle exhaust (31.1%), followed by coal combustion (22.4%), industrial production (18.1%), soil dust (14.3%) and others (14.1%). The contribution from vehicles had increased by 1.7 percentage points compared to 2010-2011. To examine the contribution of vehicles, power plants, and industries to $PM_{2.5}$ concentrations, $PM_{2.5}$ concentrations from these were compared with those of other primary pollutants such as NO_x ($NO+NO_2$), CO and SO_2 (Zhao et al., 2012). As shown in **Fig. S2a-d** in the Supplement, the

linear correlations of $PM_{2.5}$ with each pollutant gas (CO, NO_2 and SO_2) and their sum were positive and highly significant (R=0.40-0.88, p<0.05) during the study period, except for the relationship between $PM_{2.5}$ and NO_2 during the pre-Parade Blue period and that of $PM_{2.5}$ versus SO_2 during the Parade Blue period, both of which were positive but not significant (p>0.05). This finding is consistent with the source apportionment results that suggest traffic, power plants and industry are significant sources of $PM_{2.5}$ in Beijing. Given the importance of local vehicle emissions vs. more distant power plant and industrial emissions for Beijing's air quality, the ratio of CO/SO_2 can be used as an indicator of the contribution of local emissions to air pollution, with higher ratios indicating higher local contributions (Tang et al., 2015). Ratios of CO/SO_2 decreased (on average by 18%) from the pre-Parade Blue to Parade Blue period, and then increased abruptly on September 4th in the Post-Parade Blue period (**Fig. 4**), further suggesting the decreased amount of pollutants from local contributions. Beijing has relatively little industry but numerous automobiles, and the emissions of SO_2 are small while those of CO and NO_x are much larger (Zhao et al., 2012). Thus, traffic emission is likely to be a determining factor influencing urban CO and NO_x levels. This, in combination with a strong positive and highly significant correlation of $PM_{2.5}$ versus $CO+NO_2$ during the study period (**Fig. S2e, Supplement**), and the weak correlation of $PM_{2.5}$ versus SO_2 noted above (**Fig. S2c, Supplement**), shows that traffic emission controls should be a priority in mitigating $PM_{2.5}$ pollution in the future.

Concentrations of $PM_{2.5}$ levels in Beijing are not only driven by primary emissions but are also affected by meteorology and atmospheric chemistry operating on the primary pollutants, leading to secondary pollutant formation (Zhang et al., 2015). To quantify the likely contribution of secondary pollutant formation of $PM_{2.5}$ as a contributor to the observed changes between the Parade Blue period and pre- and post-measurements, CO provides an excellent tracer for primary combustion sources (de Gouw et al., 2009). Daily ratios of $PM_{2.5}$/CO during the Parade Blue period decreased significantly on average by 50% and 40% relative to the pre- and

post-Parade Blue periods, respectively (**Fig. 4**), which suggests that the significant reduction of $PM_{2.5}$ concentrations during the Parade Blue period was not only due to less anthropogenic primary emissions but also due to reduced secondary pollutant formation. This is further supported by our measured results at urban site 22, where average SIA concentrations comprised 20-29% of average $PM_{2.5}$ mass over the three periods, and decreased significantly during the Parade Blue period compared with those during the pre- and post-Parade Blue periods (**Table 1**). Significant reduction of concentrations of precursor gases (e.g. NO_2, SO_2 and NH_3) at the city scale is likely to be the major reason for such reduced secondary pollutant formation. In addition, lower concentrations of sulfate and nitrate during the Parade Blue period might also be caused by lower oxidation rates of SO_2 and NO_x. The sulfur oxidation ratio ($SOR=nSO_4^{2-}/(nSO_4^{2-}+nSO_2)$) and the nitrogen oxidation ratio ($NOR=nNO_3^-/(nNO_3^-+nNO_2)$) (*n* refers to the molar concentration) are indicators of secondary pollutant transformation in the atmosphere. Higher values of SOR and NOR imply more complete oxidation of gaseous species to sulfate- and nitrate-containing secondary particles (Sun et al., 2006). To understand the potential change in the degree of oxidation of sulfur and nitrogen, we used daily concentrations of SO_4^{2-} and NO_3^- measured at urban site 22 (located at west campus of China Agricultural University) and the MEP-reported concentrations of SO_2 and NO_2 at the Wanliu monitoring station to calculate the SOR and NOR values. This is because these two sites, only 7 km apart (**Fig. S3, Supplement**), experience similar pollution climates. The average values of SOR and NOR were 0.64 and 0.04 during the pre-Parade Blue period, 0.47 and 0.03 during the Parade Blue period, and 0.48 and 0.07 during the Post-Parade Blue period, respectively. (**Fig. S4, Supplement**). Compared with the pre- and post-Parade Blue periods, slightly reduced values of SOR and NOR during the Parade Blue period suggests a possible minor role for changes in the extent of photochemical oxidation in secondary transformation.

Ammonia is the primary alkaline trace gas in the atmosphere. In ammonia-rich environments, NH_4HSO_4 and $(NH_4)_2SO_4$ are sequentially formed, and the surplus

NH_3 that does not react with H_2SO_4 can form NH_4NO_3 (Wang et al., 2005). In both the pre-Parade Blue and Parade Blue periods, NH_4^+ was strongly correlated with SO_4^{2-} (**Fig. S5 a** and **c, Supplement**) and [SO_4^{2-}+NO_3^-] (**Fig. S5 b** and **d, Supplement**), and the regression slopes were both 0.87 during the pre-Parade Blue period, 0.97 and 0.91 during the Parade Blue period, and 1.13 and 0.79 during the post-Parade Blue period, respectively. These results indicate almost complete neutralization of acidic species (HNO_3 and H_2SO_4) by NH_3 in $PM_{2.5}$ during these three periods especially in the Parade Blue period. In this way, SIA concentrations from these sources could not be further reduced during the Parade Blue period unless NH_3 emissions were reduced more than those of SO_2 and NO_x.

4.2 Impact of traffic NH_3 emission on urban NH_3 concentration

The sources of NH_3 are often dominated by agriculture, but it may also be produced by motor vehicles due to the over-reduction of NO in catalytic converters (Kean et al., 2000). The contribution of traffic to the total NH_3 emissions is estimated at approximately 2% in Europe (EEA, 2011) and 5% in the US (Kean et al., 2009). In China, NH_3 emissions from traffic rose from 0.005 Tg (contributing approximately 0.08% to total NH_3 emissions) in 1980 to 0.5 Tg (contributing approximately 5% to total emissions) in 2012 (Kang et al., 2016). Recent studies have discussed the origin of atmospheric NH_3 in Beijing city based on the $\delta^{15}N$ technique (Chang et al., 2016; Pan et al., 2016). For example, Chang et al. (2016) identified that non-agricultural sources, merged with waste and traffic NH_3 emissions, collectively accounted for approximately 50% of ambient NH_3 in urban Beijing before and after APEC summit, of which more than 20% was sourced from traffic emissions. Traffic is therefore likely to make a very significant contribution to NH_3 concentrations in urban areas of Beijing, and a strong correlation of NH_3 with traffic-related pollutants was observed (NO_x and CO) at the urban sites (Ianniello et al., 2010; Meng et al., 2011). However, this relationship has a large uncertainty because the concentrations of pollutants used to establish the relationship were measured at 'background' urban sites some distance from major roads, and other urban sources such as decaying organic matter

may contribute. In the present study, strong and significant correlations were observed between NH_3 and NO_2 concentrations measured on the 5th ring road during all three periods (**Fig. 5**). In addition, compared with the averages for the three ring roads during the pre- and/or post-Parade Blue periods, the average NH_3 concentrations during the Parade Blue period decreased significantly owing to traffic reduction measures (**Fig. 2A c**). These results provide strong evidence that traffic is an important source of NH_3 in Beijing. In addition to period-to-period temporal changes, the mean NH_3 concentration at all road sites was 1.3 and 1.9 times that at all non-road sites during the Parade Blue period and post-Parade Blue period, respectively (**Fig. 2A**). Moreover, during the post-Parade Blue period the measured NH_3 concentrations on the three ring roads (28.3 ± 6.4 μg m^{-3}) were twice those at the rural sites 29 and 30 (14.0 ± 1.6 μg m^{-3}) affected by intense agricultural NH_3 emissions. These results, along with the fact that urban Beijing has a higher relative on-road vehicle density and almost no agricultural activity, suggest that NH_3 emission and transport from local traffic were the main contributors to high urban NH_3 concentrations. Based on a mileage-based NH_3 emission factors of 28 ± 5 (assumed as the lower limit, Chang et al., 2016) and 230 ± 14.1 mg km^{-1} (assumed as the upper limit, Liu et al., 2014) for light-duty gasoline vehicles, a population of 5.61 million vehicles (average mileage 21849 km vehicle^{-1} yr^{-1}) in Beijing would produce approximately 3.4-28 kt NH_3 in 2015, which likely declined by up to 4.7-38 t NH_3 day^{-1} during the Parade Blue period, given that the traffic load decreased by half with the implementation of the odd-and-even car ban policy. For accurately determining NH_3 emissions, however, further study on NH_3 emission factors for vehicles and other sources is warranted.

4.3 Impact of meteorological conditions and long-range air transport

Meteorological conditions strongly regulate near-surface air pollutant concentrations (Liu et al., 2015), contributing the largest uncertainties to the evaluation of the effects of emission controls on pollutant reduction. Here we first compared the

meteorological data obtained during the Parade Blue period with those from the pre- and/or post-Parade Blue periods in Beijing and other cities over North China. In Beijing, neither wind speed (WS) nor relative humidity (RH) differed significantly between non-Parade Blue (the pre- and post-Parade Blue) and the Parade Blue periods, while temperature (*T*) showed a significant but small decrease with time (**Fig. 6**). Similarly, there were small and non-significant changes in *T*, WS and RH between the pre-Parade Blue and Parade Blue periods for emission control regions (excluding Beijing) and for non-emission control regions in China. These results suggest that the period-to-period changes in *T*, WS and RH may have only a minor impact on $PM_{2.5}$, PM_{10}, NO_2, SO_2 and CO concentrations in the emission control regions (**Fig. 3**). In contrast, a higher temperature during the Parade Blue period, compared to the post-Parade Blue period, can in part explain the corresponding higher NH_3 concentrations measured at NRS, due to increased NH_3 emissions from biological sources such as humans, sewage systems and organic waste in garbage containers (Reche et al., 2012).

Surface weather maps of China (**Fig. S6, Supplement**) and North China (**Fig. 7**) showed an apparent change of wind field over Beijing and its surrounding regions during the Parade Blue period compared with the other two periods. As shown in **Fig. 7**, Beijing was located at the rear of a high pressure system within the southeast/south flow or in a high-pressure area when the wind was weak (< 3 m s^{-1}), and at the base of the Siberian high pressure system when influenced by a weak cold front and easterly wind (> 4 m s^{-1}) in the non-Parade (pre- or post-Parade) Blue and Parade Blue periods, respectively. The former weather condition (non-Parade Blue periods) was conducive to pollutant convergence and the latter (Parade Blue period) was conducive to pollutant dispersion. A further analysis of wind rose plots (**Fig. 8a**) showed that northerly winds, with similar wind speeds, dominated all three periods. Northerly/northwesterly winds in Beijing bring relatively clean air due to a lack of heavy industry in the areas north/northwest of Beijing. Winds during the pre- and post-Parade Blue periods were occasionally from the south, southeast and east of

Beijing, where the regions (e.g. Hebei, Henan and Shandong provinces) are characterized by substantially higher anthropogenic emissions of air pollutants such as NH_3, NO_x, SO_2 and aerosols (Zhang et al., 2009, 2010; Gu et al., 2012). Also as mentioned earlier, the topography of the mountains to the West and North of Beijing effectively traps the polluted air over Beijing during southerly airflow, suggesting that the southerly wind during non-Parade Blue periods may enhance air pollution in Beijing. Wet scavenging from precipitation, although often important in summer (Yoo et al., 2014), probably played a minor role in changing the concentrations of pollutants given the low and comparable precipitation over Beijing and surrounding areas during the study periods (**Fig. 8**). For example, the total precipitation in Beijing was comparable between the pre-Parade Blue and Parade Blue periods (38.9 versus 34.4 mm) (**Fig. 8b**). In addition, we compared daily mean mixing layer height (MLH) in Beijing during the study period (**Fig. 9a**). The daily mean MLH in Beijing was approx. 37% higher during the Parade Blue period (1777 m) than the pre-Parade (1301 m) and post-Parade (1296 m) Blue periods (**Fig. 9b**, $p = 0.08$). Since the MLH during Parade Blue was higher than that during non-Parade Blue periods, the horizontal and vertical diffusion conditions during the Parade Blue period were better than the other two periods.

Changes in meteorological conditions often lead to changes in regional pollution transport and ventilation. It has been shown that regional transport from neighboring Tianjin, Hebei, Shanxi, and Shandong Provinces can have a significant impact on Beijing's air quality (Meng et al., 2011; Zhang et al., 2015). Model calculations by Zhang et al. (2015) suggested that about half of Beijing's $PM_{2.5}$ pollution originates from sources outside of the city. Trajectory analysis in previous studies revealed that the air mass from south and southeast regions of Beijing led to high concentrations of NH_3, NO_x, $PM_{2.5}$ and secondary inorganic ions during summertime (Ianniello et al., 2010; Wang et al., 2010; Sun et al., 2015). The 72-hour back trajectories during the three measurement periods, shown in **Fig. 10**, were classified into 4 sectors according to air mass pathways: the west pathway over southern Mongolia, western

Inner Mongolia, and SinKiang, the north pathway over Inner Mongolia, Heilongjiang and north Hebei Provinces, the east pathway mainly over northeast Hebei province and Tianjin municipality, and the south sector over the south Hebei and Shandong provinces. The results indicated that transport of regional pollution from the south sector occurred during the pre-Parade Blue period (38%) and the post-Parade Blue period (18% for $PM_{2.5}$ sampling days and 29% for NH_3 sampling days) but there was no transport of regional pollution during the Parade Blue period. As the south of Hebei province contains heavily polluting industry and intensive agriculture (Zhang et al., 2009; Sun et al., 2015), the absence of transport of air masses from the south sector is likely at least partly responsible for lower concentrations of the five reported pollutants ($PM_{2.5}$, PM_{10}, NO_2, SO_2 and CO) during the Parade Blue period. As for NH_3, however, average concentration at NRS were slighter higher in the Parade Blue period than in the post-Parade Blue period (**Fig. 2A c**), indicating that surface levels of NH_3 were less influenced by southern air masses. Much of the airflow travelled over Tianjin municipality during the Parade Blue period (32%) compared to that during the post-Parade Blue period (19%) (**Fig. 10 b**, **d**), which probably caused the high surface NH_3 concentrations in Beijing. This is because Tianjin, as one of the mega-cities in China, has high NH_3 emissions from livestock and fertilizer application (Zhang et al., 2010).

To further diagnose the impacts of meteorology on the surface air quality, we conducted a simulation using the nested GEOS-Chem atmospheric chemistry model driven by the GEOS-FP assimilated meteorological fields at 1/4°×5/16° horizontal resolution covering East Asia (70°E-140°E, 15°N-55°N) (Zhang et al., 2015; 2016). Details of the model emissions and mechanisms have been described in Zhang et al. (2016), focusing on $PM_{2.5}$ concentrations in Beijing during the Asia-Pacific Economic Cooperation Summit (APEC; November 5-11) period. We used anthropogenic emissions from the Multi-Resolution Emission Inventory of China for the year 2010 (MEIC, 2015), except for NH_3 emissions that were taken from the Regional Emission in Asia (REAS-v2) inventory (Kurokawa et al., 2013) with an

improved seasonality derived by Zhao et al. (2015).

We conducted a standard simulation with fixed anthropogenic emissions for the period of 1 August – 12 September 2015. By fixing anthropogenic emissions in the simulation, the model provides a quantitative estimate of the meteorological impacts alone before and during the Parade Blue period. For the pre-Parade period (1-19 August), the model-simulated mean $PM_{2.5}$ concentration is 62 μg m^{-3} in Beijing, comparable to the measured values (59 μg m^{-3}), but simulated NH_3 concentrations are too low (3 μg m^{-3} vs. 8.2-31.7 μg m^{-3}), probably due to missing urban NH_3 sources and the coarse model resolution (1/4°×5/16°). Here we focus on the model simulated relative changes in pollutant concentrations before and during the Parade Blue period. Model results showed that, without emission controls, the air pollutant concentrations in Beijing in the Parade Blue period relative to the pre-Parade period would be 29% lower for $PM_{2.5}$, 7% lower for NH_3, 17% lower for SO_2, 8% lower for CO and relatively no change for NO_2 (**Fig. 11a**) as a result of the different meteorological conditions as discussed above. Thus, compared with meteorological condition changes (MCC), air pollution control measures (PCM) made a greater contribution to air quality improvement (especially for $PM_{2.5}$, NO_x, and CO) in Beijing during the Parade Blue period (**Fig. 11b**).

We also conducted two sensitivity simulations ((1) with anthropogenic emissions of NH_3 reduced by 40% over Beijing and by 30% over Hebei and Tianjin; and (2) with all anthropogenic emissions including NH_3, SO_2, NO_x, CO, and primary aerosol reduced by 40% over Beijing and by 30% over Hebei and Tianjin) for the Parade Blue period (20 August-3 September) to examine the responses of $PM_{2.5}$ concentrations to emission reductions. We find that the NH_3 emission reduction (by 40% over Beijing and by 30% over Hebei and Tianjin) could decrease the mean $PM_{2.5}$ concentration in Beijing by 12% for the period, compared with 31% simulated $PM_{2.5}$ reduction if all anthropogenic emissions were reduced by the same amount. This supports our findings on the effectiveness of emission controls during the Parade Blue period as indicated in the measurements, and the high sensitivity of

586 $PM_{2.5}$ concentration in Beijing to NH_3 sources.

587

588 *4.4 Implications for regional air pollution control*

589 Besides Tianjin, Beijing city is surrounded by four provinces, Hebei, Shandong,
590 Henan and Shanxi, which all have major power plants and manufacturing industry.
591 In the INTEX-B emission inventory, the total emissions from these four provinces
592 accounted for 28.7%, 27.9%, 28.3%, and 25.0% of national emissions of $PM_{2.5}$,
593 PM_{10}, SO_2, and NO_x, respectively (Zhang et al., 2009). The 'Parade Blue' experience
594 demonstrates that, by taking appropriate but strict coordinated regional and local
595 emission controls, air quality in megacities can be significantly and quickly
596 improved.

597 China is not the first country to use temporal emission control strategies. In 1996, the
598 city of Atlanta, for example, adopted a series of actions to reduce traffic volume and
599 significantly improved air quality during the Atlanta Olympic Games (Tian and
600 Brimblecombe, 2008; Peel et al., 2010). We also should note that most of these
601 emission control strategies have not been maintained after the Olympic Games. In
602 the long term, temporary emission control strategies will not improve regional air
603 quality conditions and we should seek better ways towards sustainable development.
604 Integrated emission reduction measures are therefore necessary, but meteorological
605 conditions also need to be considered for a sustainable solution, as in Urumqi,
606 northwest China (Song et al., 2015). We therefore recommend further efforts to build
607 on the Parade Blue experience of successful air quality improvement in Beijing and
608 the surrounding region to improve air pollution control policies throughout China
609 and in other rapidly developing countries.

610 Chinese national SO_2 emissions have been successfully reduced by 14% from the
611 2005 level due to an SO_2 control policy (Wang et al., 2014), and nationwide controls
612 on NO_x emissions have been implemented along with the controls on SO_2 and
613 primary particles during 2011-2015. However, there is as yet no regulation or policy
614 that targets national NH_3 emissions. Future emission control policies to mitigate PM

and SIA pollution in China should, in addition to focusing on primary particles, NO_x and SO_2, also address NH_3 emission reduction from both agricultural and non-agricultural sectors (e.g. traffic sources) in particular when NH_3 becomes key to $PM_{2.5}$ formation (Liu et al., 2013; Wu et al ., 2016; Xu et al., 2016).

Conclusions

We have presented atmospheric concentrations of NH_3, NO_2, $PM_{2.5}$ and associated inorganic water-soluble ions before, during, and after the Parade Blue period measured at thirty-one *in situ* sites in and outside Beijing, and daily concentrations of $PM_{2.5}$, PM_{10}, NO_2, SO_2 and CO in 291 cities in China during the pre-Parade Blue and Parade Blue periods released by the Ministry of Environmental Protection (MEP) of China. Our unique study examines temporal variations at local and regional scales across China and the relative role of the emission controls and meteorological conditions, as well as the contribution of traffic, to NH_3 levels in Beijing based on the first direct measurements of NH_3 and NO_2 concentrations at road sites. The following major findings and conclusions were reached:

The concentrations of NH_3 and NO_2 during the Parade Blue period at the road sites in different areas of Beijing decreased significantly by 12-35% and 34-59% respectively relative to the pre-and post-Parade Blue measurements, while those at the non-road sites showed an increase of 15% for NH_3 and reductions of 33% and 42% for NO_2. Positive and significant correlations were observed between NH_3 and NO_2 concentrations measured at road sites. Taken together, these findings indicate that on-road traffic is an important source of NH_3 in the urban Beijing. Daily concentrations of $PM_{2.5}$ and secondary inorganic aerosols (sulfate, ammonium, and nitrate) at the urban and rural sites both decreased during the Parade Blue period, which was closely related to controls of secondary aerosol precursors (NH_3, SO_2 and NO_x) and/or reduced secondary pollutant formation.

During the Parade Blue period, daily concentrations of air pollutants ($PM_{2.5}$, PM_{10}, NO_2, SO_2 and CO) in 291 cities obtained from the national air quality monitoring

network showed large and significant reductions of 34-72% in Beijing, small reductions of 1-32% in emission control regions (excluding Beijing), and slight increases (6-16%) in non-emission control regions that in some cases were significant, which reflects the positive effects of emission controls on air quality and suggests that the extent of air quality improvement was directly associated with the reduction intensities of pollutant emissions.

A detailed characterization of meteorological parameters and regional transport demonstrated that the good air quality in Beijing during the Parade Blue period was the combined result of emission controls, meteorological effects and the absence of transport of air masses from the south of Beijing. Thus, the net effectiveness of emission controls was investigated further by excluding the effects of meteorology in model simulations, which showed that emission controls can contribute reductions of pollutant concentrations of nearly 60% for $PM_{2.5}$, 109% for NO_2, 80% for CO, 53% for NH_3 and 50% for SO_2. This result showed that emission controls played an dominant role in air quality improvement in Beijing during the Parade Blue period.

Acknowledgments

We thank Lu Li, Hao Tianxiang, Wang Sen and Wang Wei for their assistance during the field measurements. This work was financially supported by the 973 project (2014BC954200) and the National Natural Science Foundation of China (41425007, 31421092).

Author Contributions

X.L. and F.Z. designed the research. X.L., W.X., W.S., Y.Z., D.Y., D.W. Z.W. and A.T. conducted the research (collected the data and performed the measurements). W.X., W.S., Z.L. and X.L. wrote the manuscript. All authors were involved in the discussion and interpretation of the data as well as the revision on the manuscript.

673 **References**

674 Chan, C. K., and Yao, X. H.: Air pollution in mega cities in China. Atmos. Environ.,
675 42, 1-42, doi:10.1016/j.atmosenv.2007.09.003, 2008.
676 Chang, Y. H., Liu, X. J., Deng, C. R., Dore, A. J., and Zhuang, G. S: Source
677 apportionment of atmospheric ammonia before, during, and after the 2014 APEC
678 summit in Beijing using stable nitrogen isotope signatures, Atmos. Chem. Phys.,
679 16, 11635–11647, doi:10.5194/acp-16-11635-2016, 2016.
680 Chen, C., Sun, Y. L., Xu, W. Q., Du, W., Zhou, L. B., Han, T. T., Wang, Q. Q., Fu,
681 P. Q., Wang, Z. F., Gao, Z. Q., Zhang, Q., and Worsnop, D. R.: Characteristics
682 and sources of submicron aerosols above the urban canopy (260 m) in Beijing,
683 China, during the 2014 APEC summit, Atmos. Chem. Phys., 15, 12879-12895,
684 doi:10.5194/acp-15-12879-2015, 2015.
685 Chen, R. S., De Sherbinin, A., Ye, C., and Shi, G. Q.: China's Soil Pollution: Farms
686 on the Frontline, Science, 344, 691-691, 2014.
687 Davis, D. L., Bell, M. L., and Fletcher, T.: A Look Back at the London Smog of 1952
688 and the Half Century Since, Environ. Health Persp., 110, A734-A735, 2002.
689 de Gouw, J. A., Welsh-Bon, D., Warneke, C., Kuster, W. C., Alexander, L., Baker, A.
690 K., Beyersdorf, A. J., Blake, D. R., Canagaratna, M., Celada, A. T., Huey, L. G.,
691 Junkermann, W., Onasch, T. B., Salcido, A., Sjostedt, S. J., Sullivan, A. P., Tanner,
692 D. J., Vargas. O., Weber, R. J., Worsnop, D. R., Yu, X. Y., and Zaveri, R.:
693 Emission and chemistry of organic carbon in the gas and aerosol phase at a
694 sub-urban site near Mexico City in March 2006 during the MILAGRO study,
695 Atmos. Chem. Phys., 9, 3425-3442, 2009.
696 Draxler, R. R., and Hess, G.: Description of the HYSPLIT4 modeling system, Air
697 Resources Laboratory, Silver Spring, Maryland,1997.
698 Draxler, R., Stunder, B., Rolph, G., Stein, A., and Taylor, A.: HYSPLIT4 user’s guide,
699 version 4, report, NOAA, Silver Spring, Md, 2012.
700 EEA (European Environment Agency): Air Quality in Europe-2011 Report,
701 Technical Report 12/2011, EEA, Kopenhagen, 2011.

Gu, B. J., Ge, Y., Ren, Y., Xu, B., Luo, W. D., Jiang, H., Gu, B. H., and Chang, J.: Atmospheric reactive nitrogen in China: Sources, recent trends, and damage costs. Environ. Sci. Technol., 46, 9240-9247, doi:10.1021/es301446g, 2012.

Guo, J. H., Liu, X. J., Zhang, Y., Shen, J. L., Han, W. X., Zhang, W. F., Christie, P., Goulding, K., Vitousek, P., Zhang, F. S.: Significant soil acidification in major Chinese croplands, Science, 327, 1008-1010, doi: 10.1126/science.1182570, 2010.

Haagen-Smit, A.J.: Chemistry and physiology of Los Angeles smog, Ind. Eng. Chem., 44, 1342-1346, doi:10.1021/ie50510a045, 1952.

Holzworth, G. C.: Estimates of mean maximum mixing depths in the contiguous United States, Monthly Weather Review, 92, 235-242, 1964.

Holzworth, G. C.: Mixing depths, wind speeds and air pollution potential for selected locations in the United States, Journal of Applied Meteorology, 6,1039-1044, 1967.

Huang, R.-J., Zhang, Y., Bozzetti, C., Ho, K.-F., Cao, J.-J., Han, Y., Daellenbach, K. R., Slowik, J. G., Platt, S. M., Canonaco, F., Zotter, P., Wolf, R., Pieber, S. M., Bruns, E. A., Crippa, M., Ciarelli, G., Piazzalunga, A., Schwikowski, M., Abbaszade, G., Schnelle-Kreis, J., Zimmermann, R., An, Z., Szidat, S., Baltensperger, U., Haddad, I. E., and Prevot, A. S. H.: High secondary aerosol contribution to particulate pollution during haze events in China, Nature, 514, 218-222, 2014.

Ianniello, A,, Spataro, F,, Esposito, G,, Allegrini, I,, Rantica, E,, Ancora, M. P., Hu, M., and Zhu, T.: Occurrence of gas phase ammonia in the area of Beijing (China), Atmos. Chem. Phys., 10, 9487-9503, doi:10.5194/acp-10-9487-2010, 2010.

Kang, Y. N., Liu, M. X., Song, Y., Huang, X., Yao, H., Cai, X. H., Zhang, H. S., Kang, L., Liu, X. J., Yan, X. Y., He, H., Zhang, Q., Shao, M., and Zhu, T.: High-resolution ammonia emissions inventories in China from 1980 to 2012, Atmos. Chem. Phys., 16, 2043-2058, doi: 10.5194/acp-16-2043-2016, 2016.

Kean, A. J., and Harley, R. A.: On-road measurement of ammonia and other motor vehicle exhaust emissions, Environ. Sci. Technol., 34, 3535-3539,

731 doi:10.1021/es991451q, 2000.
732 Kean, A. J., Littlejohn, D., Ban-Weiss, G. A., Harley, R. A., Kirchstetter, T. W., and
733 Lunden, M. M.: Trends in on-road vehicle emissions of ammonia, Atmos.
734 Environ., 43, 1565-1570, doi: 10.1016/j.atmosenv.2008.09.085, 2009.
735 Liu, T. Y., Wang, X. M., Wang, B. G., Ding, X., Deng, W., Lu, S. J., and Zhang, Y.
736 L.: Emission factor of ammonia (NH_3) from on-road vehicles in China: tunnel
737 tests in urban Guangzhou, Environ. Res. Lett., 9, 064027,
738 doi:10.1088/1748-9326/9/6/064027, 2014.
739 Liu, X. J., Zhang, Y., Han, W. X., Tang, A. H., Shen, J. L., Cui, Z. L., Vitousek, P.,
740 Erisman, J. W., Goulding, K., Christie, P., Fangmeier, A., and Zhang, F. S.:
741 Enhanced nitrogen deposition over China, Nature, 494, 459-462,
742 doi:10.1038/nature11917, 2013.
743 Liu, Z. R., Hu, B., Wang, L. L., Wu, F. K., Gao, W. K., and Wang, Y. S.: Seasonal
744 and diurnal variation in particulate matter (PM_{10} and $PM_{2.5}$) at an urban site of
745 Beijing: analyses from a 9-year study, Environ. Sci. Pollut. Res., 22, 627-642,
746 doi:10.1007/s11356-014-3347-0, 2015.
747 Lu, Y. L., Song, S., Wang, R. S., Liu, Z. Y., Meng, J., Sweetman, A. J., Jenkins, A.,
748 Ferrier, R. C., Li, H., Luo, W., and Wang, T. Y.: Impacts of soil and water
749 pollution on food safety and health risks in China, Environ. Int., 77, 5-15,
750 doi:10.1016/j.envint.2014.12.010, 2015.
751 Meng, Z. Y., Lin, W. L., Jiang, X. M., Yan, P., Wang, Y., Zhang, Y. M., Jia, X. F.,
752 and Yu, X. L.: Characteristics of atmospheric ammonia over Beijing, China,
753 Atmos. Chem. Phys., 11, 6139-6151, doi:10.5194/acp-11-6139-2011, 2011.
754 MEPC (Ministry of Environmental Protection of China): Ambient air quality
755 standards (GB3095–2012), Available at: http://www.mep.gov.cn/ (accessed 29
756 February 2012).
757 Multi-Resolution Emission Inventory of China for the year 2010, Available at:
758 http://meicmodel.org (accessed 1 February 2015).
759 Pan, Y.P., Tian, S.L., Liu, D.W., Fang, Y.T., Zhu, X.Y., Zhang, Q., Zheng, B.,

760 Michalski, G., and Wang, Y.S.: Fossil fuel combustion-related emissions
761 dominate atmospheric ammonia sources during severe haze episodes: evidence
762 from ^{15}N stable isotope in size-resolved aerosol ammonium, Environ. Sci.
763 Technol., 50, 8049-8056, doi: .org/10.1021/acs.est.6b00634, 2016.
764 Parrish, D. D., Singh, H. B., Molina, L., and Madronich, S.: Air quality progress in
765 North American megacities: a review, Atmos. Environ., 45, 7015-7025,
766 doi:10.1016/j.atmosenv.2011.09.039, 2011.
767 Peel, J. L., Klein, M., Flanders, W. D., Mulholland, J. A., Tolbert, P. E., and
768 Committee, H. H. R.: Impact of improved air quality during the 1996 summer
769 Olympic games in Atlanta on multiple cardiovascular and respiratory
770 outcomes, Research Report, 148, 3-23, discussion 25-33, 2010.
771 Reche, C., Viana, M., Pandolfi, M., Alastuey, A., Moreno, T., Amato, F., Ripoll, A.,
772 and Querol, X.: Urban NH_3 levels and sources in a Mediterranean environment,
773 Atmos. Environ., 57, 153-164, doi:10.1016/j.atmosenv.2012.04.021, 2012.
774 Shen, J. L., Tang, A. H., Liu, X. J., Kopsch, J., Fangmeier, A., Goulding, K., and
775 Zhang, F. S.: Impacts of pollution controls on air Quality in Beijing during the
776 2008 Olympic Games, J. Environ. Qual., 40, 37-45, doi:10.2134/jeq2010.0360,
777 2011.
778 Song, W., Chang, Y. H., Liu, X. J., Li, K. H., Gong, Y, M., He, G. X., Wang, X. L.,
779 Christie, P., Zheng, M., Dore, A. J., and Tian, C. Y.: A multiyear assessment of air
780 quality benefits from China's emerging shale gas revolution: Urumqi as a case
781 study, Environ. Sci. Technol., 49, 2066-2072, doi:10.1021/es5050024, 2015.
782 Sun, Y. L., Zhuang, G. S., Tang, A. H., Wang, Y., and An, Z. H.: Chemical
783 Characteristics of $PM_{2.5}$ and PM_{10} in haze-fog episodes in Beijing, Environ. Sci.
784 Technol., 40, 3148-3155, doi:10.1021/es051533g, 2006.
785 Sun, Y. L., Wang, Z. F., Du, W., Zhang, Q., Wang, Q. Q., Fu, P. Q., Pan, X. L., Li,
786 J., Jayne, J., and Worsnop, D. R.: Long-term real-time measurements of aerosol
787 particle composition in Beijing, China: seasonal variations, meteorological effects,
788 and source analysis, Atmos. Chem. Phys., 15, 10149-10165,

789 doi:10.5194/acp-15-10149-2015, 2015.
790 Tang, G., Zhu, X, Hu, B., Xin, J., Wang, L., Münkel, C., Mao, G., and Wang, Y.:
791 Impact of emission controls on air quality in Beijing during APEC 2014:
792 lidarceilometer observations, Atmos. Chem. Phys., 15, 12667-12680,
793 doi:10.5194/acp-15-12667-2015, 2015.
794 Tao, Y., Yin, Z., Ye, X. N., Ma, Z., and Che, J. M.: Size distribution of
795 water-soluble inorganic ions in urban aerosols in Shanghai, Atmos. Pollut. Res., 5,
796 639-647, doi:10.5094/APR.2014.073, 2014.
797 Tian, Q. W., and Brimblecombe, P.: Managing air in Olympic cities, American
798 Journal of Environmental Sciences, 4, 439-444, 2008.
799 Wang, S. X., Xing, J., Zhao, B., Jang, C., Hao, J. M. Effectiveness of national air
800 pollution control policies on the air quality in metropolitan areas of China. J.
801 Environ. Sci., 26, 13-22, doi: 10.1016/S1001-0742(13)60381-2, 2014.
802 Wang, T., Nie, W., Gao, J., Xue, L. K., Gao, X. M., Wang, X. F., Qiu, J., Poon, C.
803 N., Meinardi, S., Blake, D., Wang, S. L., Ding, A. J., Chai, F. H., Zhang, Q. Z.,
804 and Wang, W. X.: Air quality during the 2008 Beijing Olympics: secondary
805 pollutants and regional impact, Atmos. Chemis. Phys., 10, 7603-7615,
806 doi:10.5194/acp-10-7603-2010, 2010.
807 Wang, W. T., Primbs, T., Tao, S., and Simonich, S. L. M.: Atmospheric Particulate
808 Matter Pollution during the 2008 Beijing Olympics, Environ Sci Technol., 43,
809 5314-5320, 2009.
810 Wang, Y., Zhuang, G., Tang, A., Yuan, H., Sun, Y., Chen, S., and Zheng, A.: The
811 ion chemistry of $PM_{2.5}$ aerosol in Beijing, Atmos. Environ., 39, 3771-3784,
812 doi:10.1016/j.atmosenv.2005.03.013, 2005.
813 Wu, Y., Gu, B., Erisman, J. W., Reis, S., Fang, Y., Lu, X., and Zhang, X.: $PM_{2.5}$
814 pollution is substantially affected by ammonia emissions in China, Environ.
815 Pollut., 218, 86-94, doi: org/10.1016/j.envpol.2016.08.027, 2016.
816 Xu, W., Zheng, K., Liu, X. J., Meng, L. M., Huaitalla, M. R., Shen, J. L., Hartung,
817 E., Gallmann, E., Roelcke, M., and Zhang, F. S.: Atmospheric NH_3 dynamics at a

typical pig farm in China and their implications, Atmos. Pollut. Res., 5, 455-463, doi:10.5094/APR.2014.053, 2014.

Xu, W., Luo, X. S., Pan, Y. P., Zhang, L., Tang, A. H., Shen, J. L., Zhang, Y., Li, K. H., Wu, Q. H., Yang, D. W., Zhang, Y. Y., Xue, J., Li, W. Q., Li, Q. Q., Tang, L., Lu, S. H., Liang, T., Tong, Y. A., Liu, P., Zhang, Q., Xiong, Z. Q., Shi, X. J., Wu, L. H., Shi, W. Q., Tian, K., Zhong, X. H., Shi, K., Tang, Q. Y., Zhang, L. J., Huang, J. L., He, C. E., Kuang, F. H., Zhu, B., Liu, H., Jin, X., Xin, Y. J., Shi, X. K., Du, E. Z., Dore, A. J., Tang, S., Collett, J. L., Goulding, K., Sun, Y. X., Ren, J., Zhang, F. S., and Liu, X. J.: Quantifying atmospheric nitrogen deposition through a nationwide monitoring network across China. Atmos. Chem. Phys, 15, 12345-12360, doi:10.5194/acp-15-12345-2015, 2015.

Xu, W., Wu, Q. H., Liu, X. J., Tang, A. H., Dore, A. J., and Heal, M. R.: Characteristics of ammonia, acid gases, and $PM_{2.5}$ for three typical land-use types in the North China Plain, Environ. Sci. Pollut. Res., 23, 1158-1172, doi:10.1007/s11356-015-5648-3, 2016.

Yoo, J. M., Lee, Y. R., Kim, D., Jeong, M. J., Stockwell, W. R., Kundu, P. K., Oh, S. M., Shin, D. B., Lee, S. J. New indices for wet scavenging of air pollutants (O_3, CO, NO_2, SO_2, and PM_{10}) by summertime rain. Atmos. Environ., 82, 226-237, doi:10.1016/j.atmosenv.2013.10.022, 2014.

Zhang, L., Liu, L. C., Zhao, Y. H., Gong, S. L., Zhang, X. Y., Henze, D. K., Capps, S. L., Fu, T. M., Zhang, Q., and Wang, Y. X.: Source attribution of particulate matter pollution over North China with the adjoint method, Environ. Res. Lett., 10, 084011, doi:10.1088/1748-9326/10/8/084011, 2015.

Zhang, L., Shao, J. Y., Lu, X., Zhao, Y. H., Hu, Y. Y., Henze, D. K., Liao, H., Gong, S. L., and Zhang, Q.: Sources and processes affecting fine particulate matter pollution over North China: an adjoint analysis of the Beijing APEC period, Environ. Sci. Technol., 50, 16, 8731–8740, 2016.

Zhang, Q., Streets, D. G., Carmichael, G. R., He, K. B., Huo, H., Kannari, A., Klimont, Z., Park, I. S., Reddy, S., Fu, J. S., Chen, D., Duan, L., Lei, Y., Wang, L.

T., and Yao, Z. L.: Asian emissions in 2006 for the NASA INTEX-B mission. Atmos. Chem. Phys., 9, 5131-5153, 2009.

Zhang, T., Cao, J. J., Tie, X. X., Shen, Z. X., Liu, S. X., Ding, H., Han, Y. M., Wang, G. H., Ho, K. F., Qiang, J., and Li, W. T.: Water-soluble ions in atmospheric aerosols measured in Xi'an, China: seasonal variations and sources, Atmos. Res., 102, 110-119, doi:10.1016/j.atmosres.2011.06.014, 2011.

Zhang, Y., Dore, A. J., Ma, L., Liu, X. J., Ma, W. Q., Cape, J. N., and Zhang, F. S.: Agricultural ammonia emissions inventory and spatial distribution in the North China Plain, Environ. Pollut., 158, 490-501, doi:10.1016/j.envpol.2009.08.033, 2010.

Zhang, Y. L., and Cao, F.: Fine particulate matter ($PM_{2.5}$) in China at a city level. Sci. Rep., 5, 14884, doi:10.1038/srep14884, 2015.

Zhao, B., Wang, P., Ma, J. Z., Zhu, S., Pozzer, A., and Li, W.: A high-resolution emission inventory of primary pollutants for the Huabei region, China, Atmos. Chem. Phys., 12, 481-501, doi:10.5194/acp-12-481-2012, 2012.

862

863 **Figure captions**

864 **Fig. 1**. Maps showing the thirty-one monitoring sites, the Beijing municipality (the
865 areas within the blue line, and the surrounding regions. Also shown are locations of
866 Tiananmen, and the 3rd, 4th, 5th and 6th ring roads.

867 **Fig. 2**. Concentrations of NH_3 (**A**) and NO_2 (**B**) during the monitoring periods at
868 different observation scales: concentrations at 31 (NH_3) or 17 (NO_2) sites (a),
869 averaged concentrations for the sites inside the 6th ring (R) road (Rd), outside the 6th
870 ring (R) road (Rd) and outside Beijing (b), averaged concentrations for the sites on
871 the 3rd, 4th and/or 5th ring roads and non-road sites (NRS) (c) (one asterisk on bars
872 denotes significant difference at p<0.05, two asterisks on bars denote significant
873 difference at p<0.01).

874 **Fig. 3**. Comparison of $PM_{2.5}$, PM_{10}, NO_2, SO_2 and CO concentrations between
875 non-Parade Blue periods (the pre- and post-Parade Blue periods) and Parade Blue
876 period at Beijing, cities in emission control regions (excluding Beijing) and other
877 cities in non-emission control regions (one asterisk on bars denotes significant
878 difference at p<0.05, two asterisks on bars denote significant difference at p<0.01).

879 **Fig. 4**. Daily values of AQI and daily ratios of CO to SO_2 concentrations and of
880 $PM_{2.5}$ to CO concentrations in Beijing during the pre-Parade Blue, Parade Blue and
881 post-Parade Blue periods.

882 **Fig. 5**. Correlations between NO_2 and NH_3 concentrations measured on the 5th ring
883 road in Beijing during the pre-Parade Blue, Parade Blue, and post-Parade Blue
884 periods.

885 **Fig. 6**. Comparison of wind speed (WS), relative humidity (RH) and temperature (T)
886 between the Parade Blue period and non-Parade Blue periods (the pre-Parade Blue
887 and post-Parade Blue periods) in Beijing, emission control regions (excluding
888 Beijing) and other cities in non-emission control regions (two asterisk on bars
889 denotes significant difference at p<0.01).

Fig. 7. Mean sea level pressure (unit: hPa) and mean wind field at 10 m height (unit: m/s) during the pre-Parade Blue (a), Parade Blue (b) and post-Parade Blue (c) periods in Beijing and North China. The color bar denotes air pressure (unit: hPa) and arrows reflect wind vector (unit: m s^{-1}).

Fig. 8. The frequency distributions of wind directions and speeds (color demarcation) (a), and daily precipitation amount (b) in Beijing city during the pre-Parade Blue, Parade Blue, and post-Parade Blue periods.

Fig. 9. Dynamics of daily mean atmospheric mixing layer height (MLH) in Beijing from 3 August to 30 September 2015 (a) and comparison of MLH means during the pre-Parade Blue, Parade Blue and post-Parade Blue periods (b).

Fig. 10. 72-h backward trajectories for 100 m above ground level in Beijing city during the pre-Parade Blue period (1 to 19 August 2015) (a), the Parade Blue period (20 August to 3 September 2015) (b), and the post-Parade Blue period (4 to 30 September 2015) (c), and for sampling duration of NH_3 (8 to 19 September 2015) in the post-Parade Blue period (d).

Fig. 11 Effect of meteorological condition change (MCC, simulated by a GEOS-Chem chemical transport model) and pollution control measures (PEM, measured by monitoring stations) to relative concentrations of CO, NO_2, SO_2, NH_3 and $PM_{2.5}$ (a) and relative contribution of MCC and PEC to major pollutant mitigation (b) in Beijing during the Parade Blue period.

Figure 1

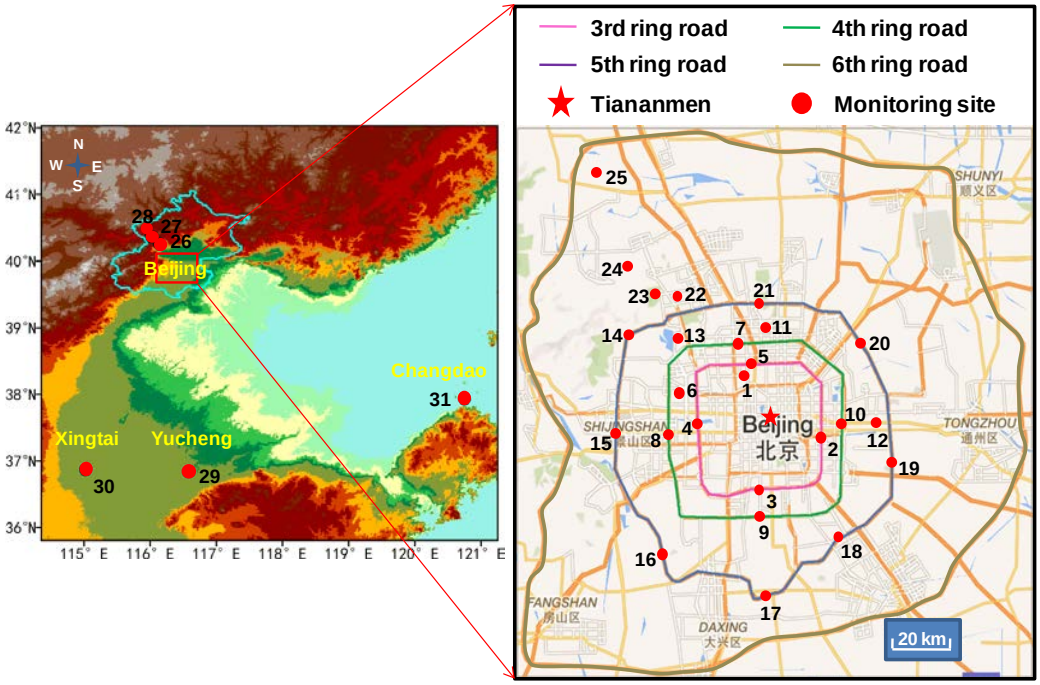
3rd ring road
4th ring road
5th ring road
6th ring road
Tiananmen
Monitoring site
42°N
41°N
40°N
39°N
38°N
37°N
36°N
115° E
116° E
117° E
118° E
119° E
120° E
121° E
N
W
E
S
Beijing
Changdao
Xingtai
Yucheng
Beijing
北京
SHUNYI
TONGZHOU
DAXING
20 km

Figure 2

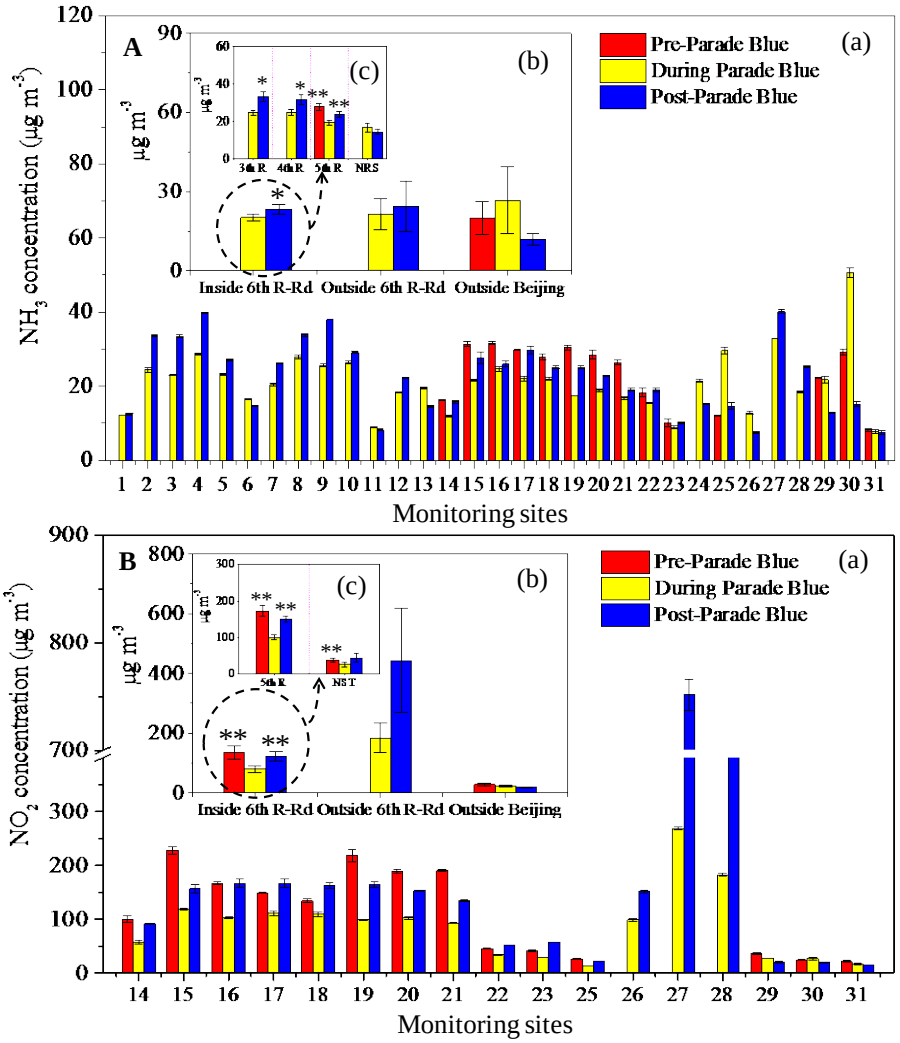
A
(a)
(b)
(c)
Pre-Parade Blue
During Parade Blue
Post-Parade Blue
NH3 concentration (μg m-3)
μg m-3
Inside 6th R-Rd
Outside 6th R-Rd
Outside Beijing
3th R
4th R
5th R
NRS
Monitoring sites
B
(a)
(b)
(c)
Pre-Parade Blue
During Parade Blue
Post-Parade Blue
NO2 concentration (μg m-3)
μg m-3
Inside 6th R-Rd
Outside 6th R-Rd
Outside Beijing
5th R
NST
Monitoring sites

945

946 **Figure 3**

947

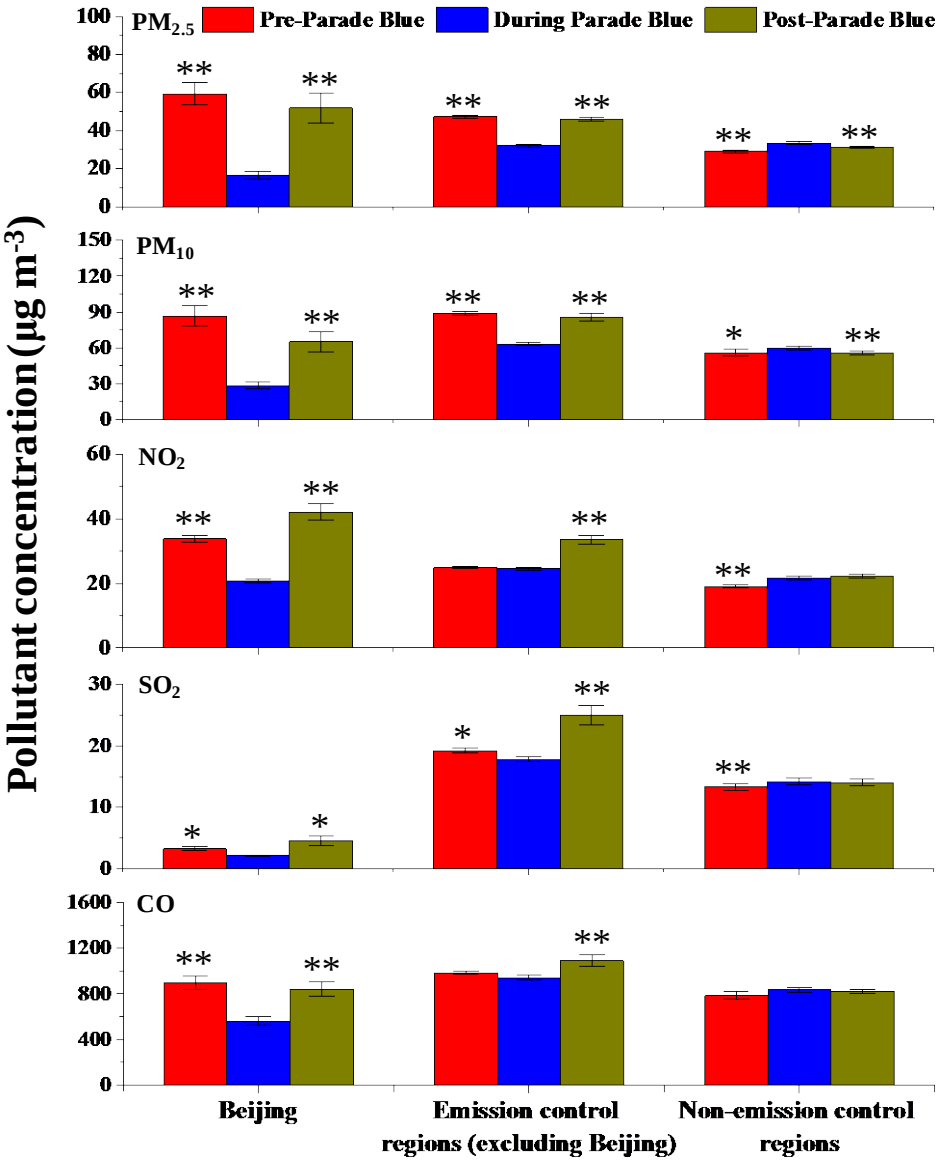

948

949

950

951

952

953

954

955

Figure 4

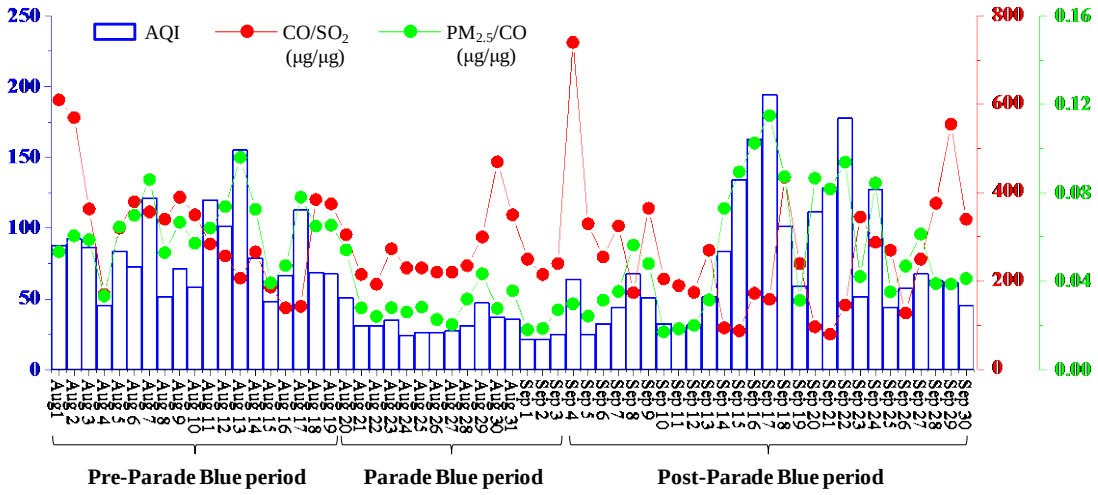
AQI
CO/SO2 (μg/μg)
PM2.5/CO (μg/μg)
250
200
150
100
50
0
800
600
400
200
0
0.16
0.12
0.08
0.04
0.00
Pre-Parade Blue period
Parade Blue period
Post-Parade Blue period

Figure 5

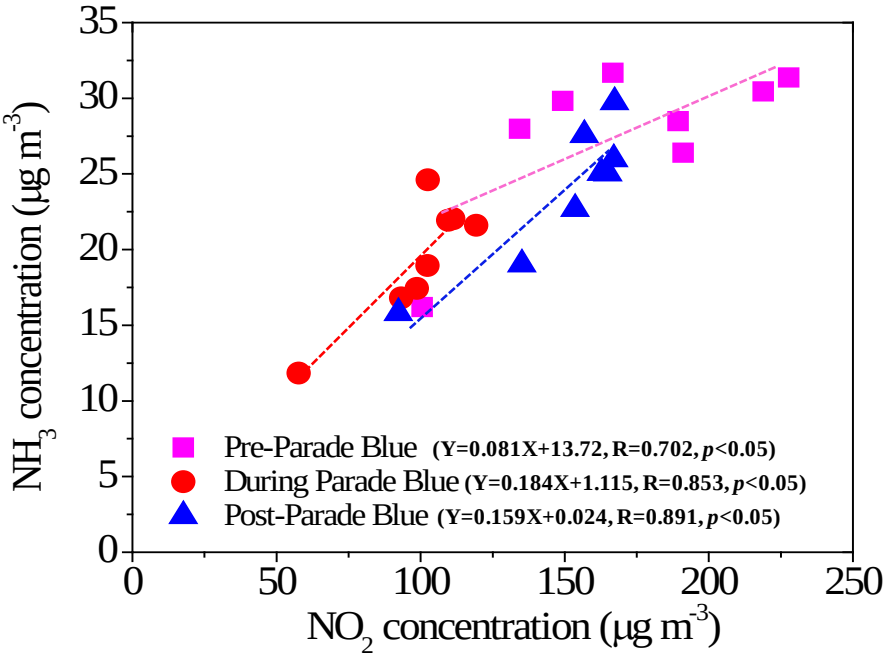
35
30
25
20
15
10
5
0
0
50
100
150
200
250
NH3 concentration (μg m-3)
NO2 concentration (μg m-3)
Pre-Parade Blue (Y=0.081X+13.72, R=0.702, p<0.05)
During Parade Blue (Y=0.184X+1.115, R=0.853, p<0.05)
Post-Parade Blue (Y=0.159X+0.024, R=0.891, p<0.05)

Figure 6

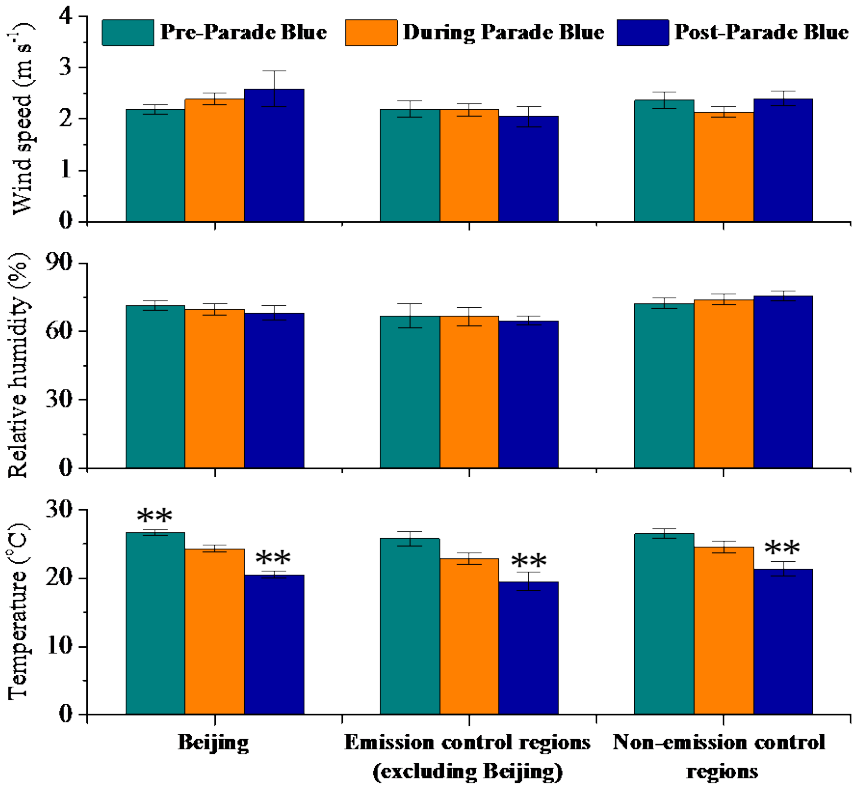
Pre-Parade Blue
During Parade Blue
Post-Parade Blue
Wind speed (m s-1)
Relative humidity (%)
Temperature (°C)
**
Beijing
Emission control regions (excluding Beijing)
Non-emission control regions

Figure 7

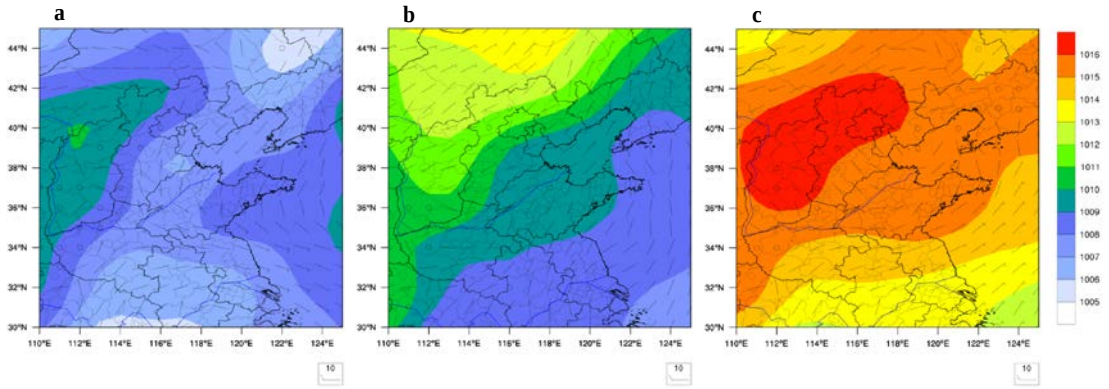
a
b
c
44°N
42°N
40°N
38°N
36°N
34°N
32°N
30°N
110°E
112°E
114°E
116°E
118°E
120°E
122°E
124°E
1016
1015
1014
1013
1012
1011
1010
1009
1008
1007
1006
1005

Figure 8

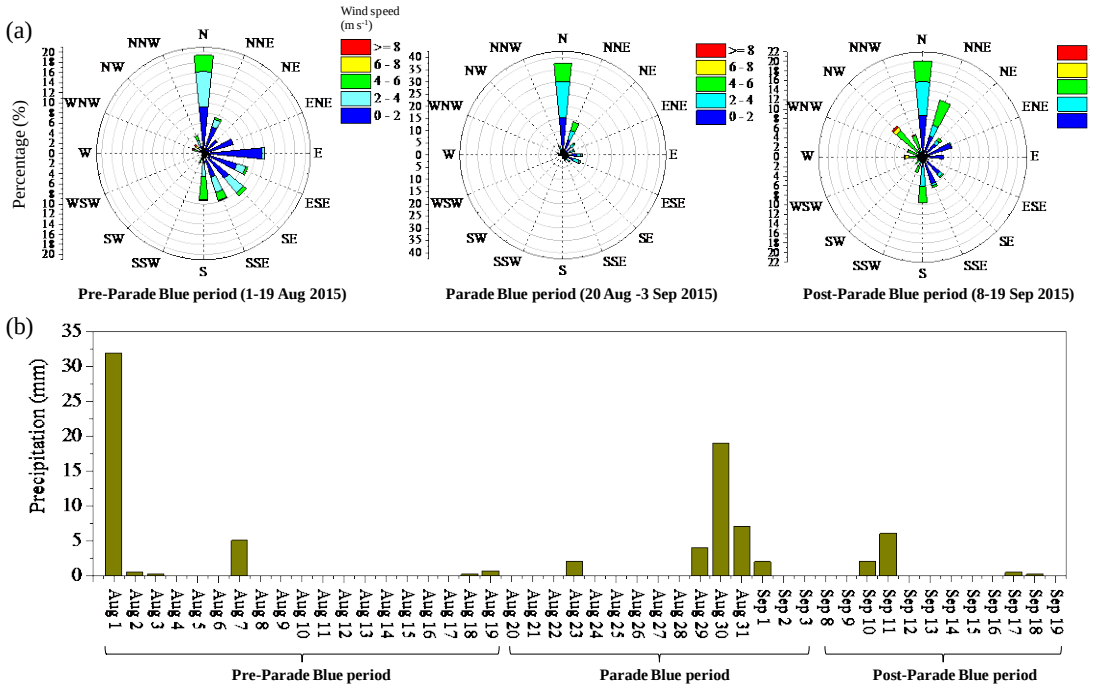
(a)
Wind speed (m s-1)
>= 8
6 - 8
4 - 6
2 - 4
0 - 2
Percentage (%)
N
NNE
NE
ENE
E
ESE
SE
SSE
S
SSW
SW
WSW
W
WNW
NW
NNW
Pre-Parade Blue period (1-19 Aug 2015)
Parade Blue period (20 Aug -3 Sep 2015)
Post-Parade Blue period (8-19 Sep 2015)
(b)
Precipitation (mm)
Pre-Parade Blue period
Parade Blue period
Post-Parade Blue period

Figure 9

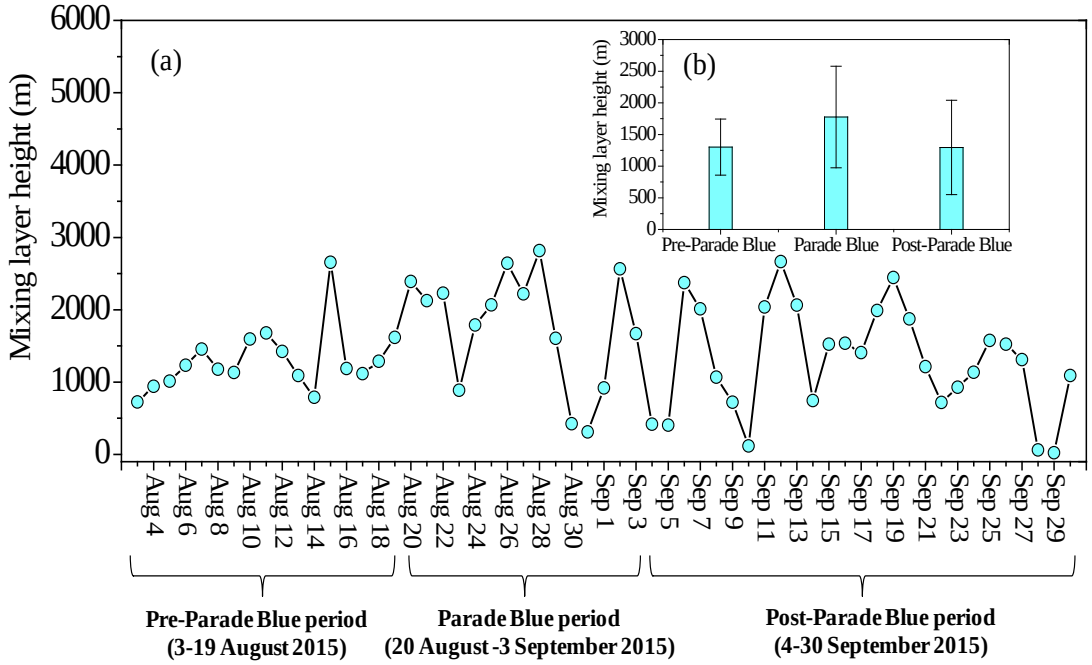
(a)
(b)
Mixing layer height (m)
6000
5000
4000
3000
2000
1000
0
3000
2500
2000
1500
1000
500
0
Pre-Parade Blue
Parade Blue
Post-Parade Blue
Aug 4
Aug 6
Aug 8
Aug 10
Aug 12
Aug 14
Aug 16
Aug 18
Aug 20
Aug 22
Aug 24
Aug 26
Aug 28
Aug 30
Sep 1
Sep 3
Sep 5
Sep 7
Sep 9
Sep 11
Sep 13
Sep 15
Sep 17
Sep 19
Sep 21
Sep 23
Sep 25
Sep 27
Sep 29
Pre-Parade Blue period
(3-19 August 2015)
Parade Blue period
(20 August -3 September 2015)
Post-Parade Blue period
(4-30 September 2015)

Figure 10

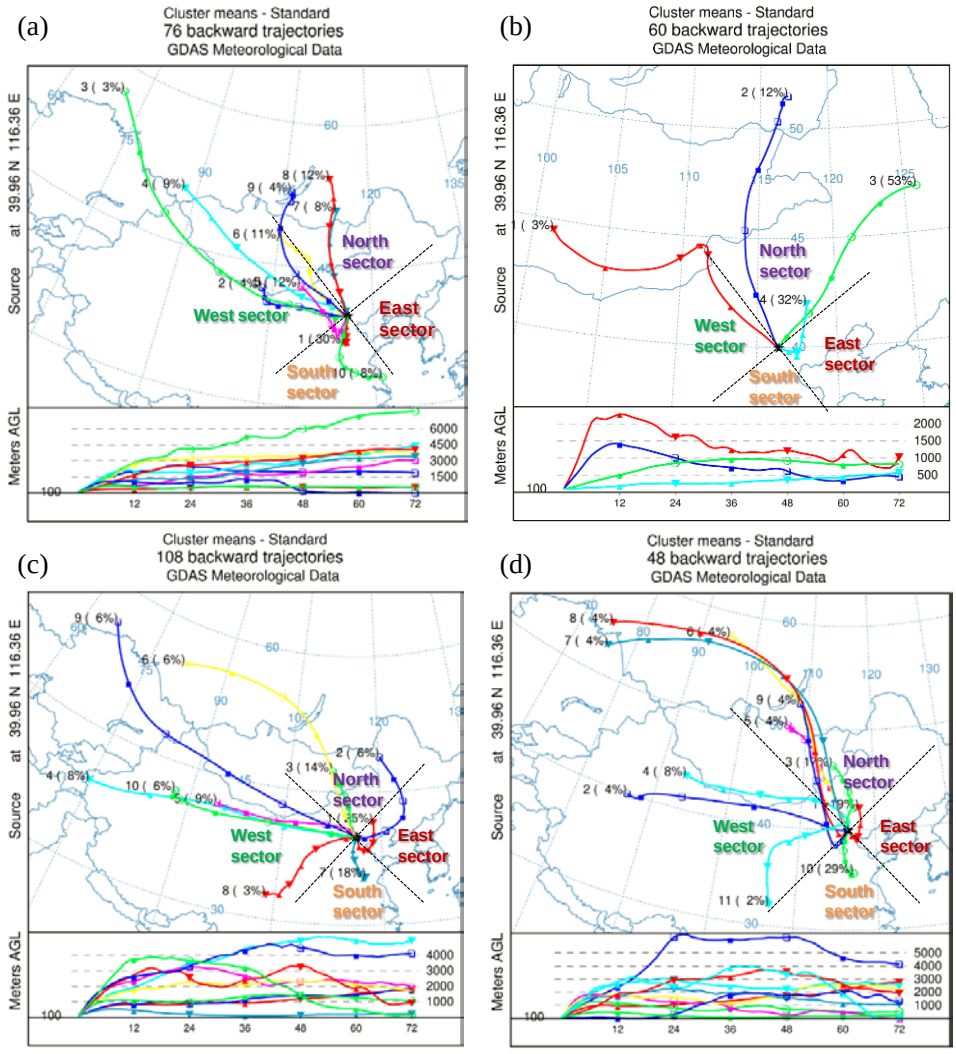
(a)
Cluster means - Standard
76 backward trajectories
GDAS Meteorological Data
North sector
West sector
East sector
South sector
Source at 39.96 N 116.36 E
Meters AGL
(b)
Cluster means - Standard
60 backward trajectories
GDAS Meteorological Data
North sector
West sector
East sector
South sector
Source at 39.96 N 116.36 E
Meters AGL
(c)
Cluster means - Standard
108 backward trajectories
GDAS Meteorological Data
North sector
West sector
East sector
South sector
Source at 39.96 N 116.36 E
Meters AGL
(d)
Cluster means - Standard
48 backward trajectories
GDAS Meteorological Data
North sector
West sector
East sector
South sector
Source at 39.96 N 116.36 E
Meters AGL

Figure 11

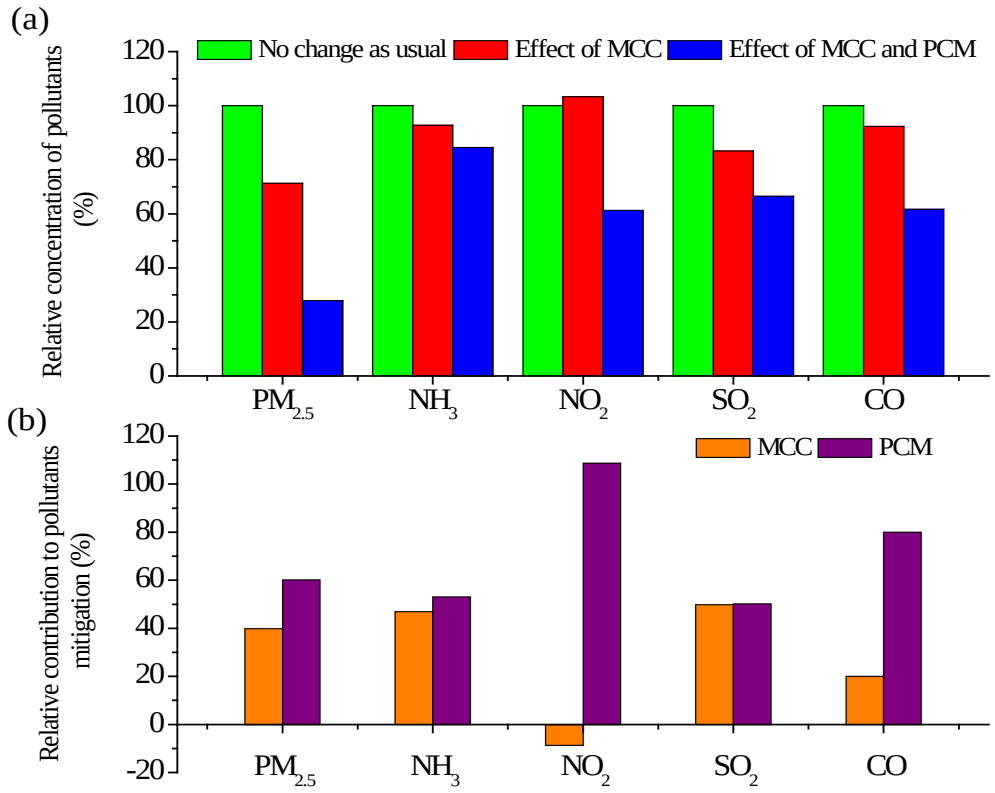
(a)
No change as usual
Effect of MCC
Effect of MCC and PCM
Relative concentration of pollutants (%)
120
100
80
60
40
20
0
PM2.5
NH3
NO2
SO2
CO
(b)
MCC
PCM
Relative contribution to pollutants mitigation (%)
120
100
80
60
40
20
0
-20
PM2.5
NH3
NO2
SO2
CO

1096 **Table 1. Mean (SE) ambient concentrations of $PM_{2.5}$ and associated ionic**

1097 **components at the urban and rural sites.**

	Urban site (Site 22) in Beijing			Rural site (Site 29) in Shandong			Rural site (Site 30) in Hebei		
	Pre-PBP (n=11)	PBP[a] (n=15)[b]	Post-PBP (n=15)	Pre-PBP (n=6)	PBP (n=5)	Post-PBP (n=10)	Pre-PBP (n=6)	PBP (n=5)	Post-PBP (n=8)
$PM_{2.5}$	72.37 (7.36)**	37.23 (5.37)	58.49 (7.99)	90.27 (8.53)*	53.84 (11.37)	55.30 (7.45)	38.73 (5.17)	29.44 (6.55)	59.73 (16.35)
NO_3^-	2.07 (0.60)	0.85 (0.15)	6.27 (1.72)**	4.21 (1.71)	1.22 (0.22)	5.56 (1.03)**	0.58 (0.22)	1.02 (0.05)	3.46 (0.81)*
SO_4^{2-}	13.26 (2.85)**	3.79 (0.69)	10.92 (2.94)	25.53 (3.36)*	11.55 (3.20)	14.80 (2.84)	9.57 (1.07)*	6.04 0.65	8.21 0.89
NH_4^+	4.62 (0.94)**	1.15 (0.26)	4.07 (1.25)	8.85 (0.91)*	3.49 (1.01)	4.32 (0.98)	2.41 (0.30)**	0.58 0.18	2.34 (0.40)**
Ca^{2+}	0.58 (0.04)**	0.38 (0.06)	0.51 (0.07)	0.29 (0.06)	0.29 (0.11)	0.23 (0.05)	0.19 (0.07)	0.12 (0.02)	0.09 (0.02)
K^+	0.30 (0.04)**	0.15 (0.02)	0.42 (0.08)**	0.76 (0.07)	0.50 (0.11)	0.99 (0.18)	0.20 (0.03)	0.18 (0.02)	0.24 (0.02)
F^-	0.17 (0.02)*	0.10 (0.01)	0.07 (0.02)	0.04 (0.03)	0.07 (0.03)	0.10 (0.04)	0.01 (0.00)	0.00 (0.00)	0.00 (0.00)
Cl^-	0.11 (0.01)	0.11 (0.01)	0.13 (0.03)	0.14 (0.03)	0.29 (0.14)	0.19 (0.06)	0.06 (0.03)	0.01 (0.00)	0.24 (0.09)*
Na^+	0.10 (0.02)	0.09 (0.02)	0.25 (0.05)**	0.25 (0.05)	0.45 (0.25)	0.42 (0.04)	0.35 (0.08)	0.52 (0.06)	0.26 (0.02)**
Mg^{2+}	0.08 (0.01)**	0.05 (0.01)	0.07 (0.01)	0.05 (0.01)	0.15 (0.12)	0.07 (0.01)	0.03 (0.00)**	0.04 (0.00)	0.04 (0.00)
SIA[c]	19.95 (3.83)**	5.78 (1.00)	21.26 (5.83)*	38.58 (3.75)**	16.26 (4.19)	24.68 (4.61)	12.56 (1.43)*	7.64 (0.81)	14.00 (1.97)*
$SIA/PM_{2.5}$ (%)	25.4 (3.2)	20.0 (4.2)	29.0 (4.8)	42.9 (2.3)	31.4 (3.7)	45.6 (4.7)	35.1 (5.2)	30.4 (5.6)	30.1 (4.4)

1098 [a] Parade Blue period. [b] Number of samples. [c] Secondary inorganic aerosol.

1099 *Significant at the 0.05 probability level. ** Significant at the 0.01 probability level.